Heavy mesons in an effective quark model with a nonlocal interaction

A. Friesen[1], Yu. Kalinovsky[1], A. Khmelev[1,2]

[1]Joint Institute for Nuclear Research. Dubna, Russia, 141980

[2] Moscow Institute of Physics and Technology, Dolgoprudny, Russia, 141700

June 2, 2025

Abstract

We discuss the properties of light and heavy mesons in the framework of a model with nonlocal interaction. We start from the Bethe-Salpeter equation, choosing the interaction kernel in a nonlocal form with the Gaussian meson vertex function. We fix the model parameters using electromagnetic and leptonic decay constants. Within this model, we consider the neutral pion transition form factor $F_{\pi\gamma}$ and apply the model to the transition form factors of heavy pseudoscalar mesons η_c and η_b. Finally, we reproduce the radiative decays of the ρ-meson and heavy quarkonia.

1 Introduction

A complete understanding of the full range of hadronic spectra from the lightest $(q\bar{q})$ to the heaviest $(Q\bar{Q})$ remains challenge. Direct calculations of hadron properties from the first principles of QCD still encounter some technical and conceptual difficulties. The use of different approaches is determined by the flavour structure of mesons. Thus, the behaviour of light flavours is determined by chiral symmetry in QCD, whereas for heavy flavours it does not play a significant role.

The spontaneous breaking of chiral symmetry in vacuum implies the existence of Goldstone bosons and the fulfillment low-energy theorems such as the GMOR, Goldberger-Treiman and KSFR relations [1, 2]. The most popular model that can describe the dynamical breaking of chiral symmetry is the NJL model, in which quarks interact through a local, chiral invariant four-fermion coupling [3]. The local nature of interaction in NJL-like models leads to the nonrenormalizability of the model, as a consequence of the divergence of loop integrals. These problems naturally disappear when considering nonlocal interaction.

For heavy flavours the chiral symmetry breaking does not play an important role. The strong dynamics of heavy quarks is more simple, since they behave like classical particles. This is why heavy quarkonia have a good description in

the framework of simple potential models (Coulomb at low distances and linear at large distances) [4]. Decent results in describing heavy mesons are reached in Lattice QCD [5] and, mainly, in the framework of nonrelativistic QCD [6].

In this work, an approach to describing properties of light and heavy mesons is developed in the framework of effective quark theory with nonlocal interaction. Models with nonlocal interaction are widely used to investigate light- and heavy- flavoured mesons [7–10] at both zero and finite temperatures [11]. The nonlocality of quark-antiquark interaction is implemented in this model via the four-momentum Gaussian form factor in the meson vertex function. The set of model parameters includes the constituent quark masses and the meson size parameters Λ_H. Integration over loop momenta in matrix elements is performed using the alpha representation, which reduces all matrix elements to the computation of simple integrals over scale variables.

The paper is organized as follows: in Section 2, the basic sentences of the model are formulated. In Section 3, the transition form factors of neutral pion and heavy pseudoscalar mesons η_c, η_b are considered. Section 4 contains an application of the developed model to the radiative decays of the ρ meson and heavy quarkonia. Conclusions are given in the last section. Appendices A and B provide some technical details on how one-loop integrations over loop momenta are performed.

2 Basic properties of pseudoscalar and vector mesons

Mesons can be described as $q\bar{q}$ bound states using the Bethe-Salpeter equation, which in the ladder approximation has the form

$$\Gamma_H(q,P) = -\frac{4}{3} \int \frac{d^4p}{(2\pi)^4} D(q-p)\gamma_\alpha S_1(p_1)\Gamma_H(p,P)S_2(p_2)\gamma_\alpha \ . \tag{1}$$

The vertex function $\Gamma_H(q,P)$ depends on the relative momentum q, and the total momentum of the bound state P. In this paper we study the rank -1 separable model with the interaction kernel $D(q-p)$

$$D(q-p) = D_0\varphi(q^2)\varphi(p^2) \,, \tag{2}$$

where D_0 is the coupling constant and the function $\varphi(p^2)$ is related to scalar part of the Bethe - Salpeter vertex function. The vertex function $\varphi(q^2)$ in the Gaussian form $\varphi(q^2) = e^{-q^2/\Lambda_H^2}$ is used with the parameter Λ_H characterizeing the finite size of the meson.

The basic object of our study is the meson vertex function, which with the separable Anzatz of the interaction kernel Eq.(2) has the form

$$\Gamma_H(p,P) = N_H \,\varphi(p^2)\,\gamma_H \,. \tag{3}$$

with the normalization constant N_H, and the Dirac matrix γ_H defined by the meson parity. $S_i(p_i)$ is the dressed quark propagator in Euclidean space

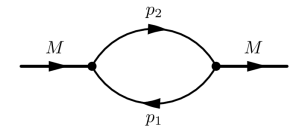$$S_i(p_i) = \frac{1}{i(p_i \cdot \gamma) + m_i}, \tag{4}$$

Figure 1: Meson polarization loop.

the momenta $p_i = p + q_i$, $q_i = b_i P$, $i = 1, 2$ and $b_1 = -m_1/(m_1 + m_2)$, $b_2 = m_2/(m_1 + m_2)$, m_i are the constituent quark masses.

The meson-quark coupling constant N_H is determined by the normalization conditions and requires the derivative of the polarization loop presented in Fig.1 over the mass operator:

$$1 = N_c \frac{P_\mu}{2P^2} \frac{\partial}{\partial P_\mu} \int \frac{d^4p}{(2\pi)^4} \text{tr} \left\{ \Gamma_H(p, P) S_1(p_1) \Gamma_H(q, P) S_2(p_2) \right\} \tag{5}$$

at the point $P^2 = -M_H^2$.

Taking into account that the derivatives of the quark propagator Eq. (4) gives $S_i(-ib_i\gamma_\mu)S_i$, the normalization conditions Eq.(5) for pseudoscalar and vector mesons can be written as:

$$1 = -i\frac{N_c N_{ps}^2}{2P^2} P^\mu \int \frac{dp}{(2\pi)^4} \varphi^2(p^2) \cdot \tag{6}$$
$$\cdot \left\{ b_1 \text{tr} \left[i\gamma_5 S_1(p_1)\gamma_\mu S_1(p_1) i\gamma_5 S_2(p_2) \right] + b_2 \text{tr} \left[S_1(p_1) i\gamma_5 S_2(p_2)\gamma_\mu S_2(p_2) i\gamma_5 \right] \right\},$$

$$1 = -i\frac{N_c N_v^2}{6P^2} P^\mu \int \frac{dp}{(2\pi)^4} \varphi^2(p^2) \epsilon^{\rho\sigma} \cdot \tag{7}$$
$$\cdot \left\{ b_1 \text{tr} \left[\gamma_\rho S_1(p_1)\gamma_\mu S_1(p_1)\gamma_\sigma S_2(p_2) \right] + b_2 \text{tr} \left[S_1(p_1)\gamma_\rho S_2(p_2)\gamma_\mu S_2(p_2) i\gamma_\sigma \right] \right\},$$

where the factor $1/3$ appears because the three transverse directions are summed. Here $\epsilon^{\mu\nu} = g^{\mu\nu} - P^\mu P^\nu/P^2$ is the polarization vector of the vector meson satisfying $\epsilon^{\mu\nu} \cdot P^\nu = 0$ and $\epsilon^{\mu\nu}\epsilon_{\mu\nu} = 3$.

The next step is to apply the model to the description of the meson properties. For pseudoscalar mesons the weak leptonic decay constant can be obtained from the matrix element of the axial current

$$f_p P^\mu := \langle 0 | \bar{\mathcal{Q}}(T^P)^T \gamma_\mu \gamma_5 \mathcal{Q} | P(p) \rangle \tag{8}$$

with the quark field spinor $\mathcal{Q} = column(u, d, s, c, b)$, and a flavour matrix T^P identifying the meson, in integral form this equation has view:

$$P^\mu f_p = N_c N_p \int \frac{dp}{(2\pi)^4} \varphi(p^2) \text{tr}\{(i\gamma_5) S_1(p_1)(\gamma_\mu\gamma_5) S_2(p_2)\}. \tag{9}$$

The vector leptonic decay can be written in the same way [10]:

$$f_v M_v \epsilon^{\mu\nu} := \langle 0 | \bar{\mathcal{Q}}(T^P)^T \gamma^\mu \mathcal{Q} | V_\nu(p) \rangle \tag{10}$$
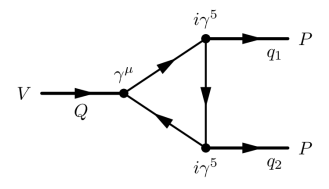
3

Figure 2: The Feynman diagram of the $\rho \to \pi\pi$ decay.

which in integral form can be expressed as a loop integral [12, 13]

$$f_{\mathrm{v}} M_{\mathrm{v}} \epsilon^{\mu\nu} = N_c N_{\mathrm{v}} \int \frac{dp}{(2\pi)^4} \varphi(p^2) \epsilon^{\mu\rho} \mathrm{tr}\{\gamma_\rho S_1(\mathrm{p}_1) \gamma_\nu S_2(\mathrm{p}_2)\}. \qquad (11)$$

To determine the decay constant for a multi-flavour configuration state such as ρ^0, it is better to use the electromagnetic decay coupling, which can be conventionally expressed via the dimensionless coupling constant g_{v} in the form $f_{\mathrm{v}} = g_{\mathrm{v}} M_{\mathrm{v}}$, where for the ρ meson the factor $\sqrt{2}$ also appears due to the meson flavour structure.

The system of equations to define the parameters of the model is complete. In the model, the constituent quark masses and the scale parameters Λ_{H} are adjustable parameters that can be obtained by fixing observables such as the meson mass and decay constants. The normalization conditions in Eqs. (6 - 7) yield the constants N_{v}, N_p, which have the meaning of meson-quark coupling constants. The evaluation of one-loop integrals that appear after taking the trace in the equations above is presented in Appendix A. Using the experimental values $m_\pi = 0.139$ GeV, $f_\pi = 0.131$ GeV, $m_\rho = 0.77$ GeV, $f_\rho = 0.2$ GeV [13, 14] and the explicit Gaussian form of the BS amplitude $\varphi(p^2) = e^{-p^2/\Lambda_H^2}$, the set of parameters for light mesons presented in Table 1 is obtained.

$m_{u(d)}$, GeV	Λ_π, GeV	N_π	Λ_ρ, GeV	N_ρ
0.223	1.14	3.724	0.75	3.612

Table 1: Basic model parameters and constants for light mesons.

To test the model, the hadronic decay of the ρ-meson $\rho \to \pi\pi$ can be studied. The Feynman diagram of the $\rho\pi\pi$ decay is shown in Fig.2 and gives the matrix element as

$$T^\mu(q_1, q_2) = N_c N_\rho N_\pi \int \frac{dp}{(2\pi)^4} \varphi(p^2) \mathrm{tr}\{\gamma_\mu S_2(p_2) i\gamma_5 S_3(p_3) i\gamma_5 S_1(p_1)\}, \qquad (12)$$

where $\varphi(p^2) = \varphi_\rho(p^2) \varphi_\pi^2(p^2)$. The matrix element can be split in two terms:

$$T^\mu(p_1, p_2) = (p_1 - p_2)^\mu f^+(t) + (p_1 + p_2)^\mu f^-(t), \qquad (13)$$

where $t = -(p_1 - p_2)^2$ and $f^-(t = M_\rho^2) = 0$, $\frac{1}{2} f^+(t = M_\rho^2) = g_{\rho\pi\pi}$.

4
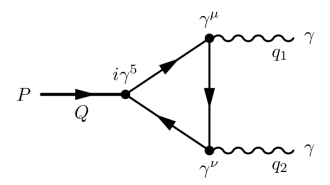
Figure 3: The Feynman diagram of electromagnetic $P \to \gamma\gamma$ decay.

The calculation technique for one-loop three-point integrals is presented in Appendix B. The decay width for the $\rho \to \pi\pi$ decay is calculated as

$$\Gamma_{\rho\pi\pi} = \frac{1}{6\pi} \frac{k^3}{M_\rho^2} g_{\rho\pi\pi}^2, \tag{14}$$

where $k = 2 \left(M_\rho^2 - 4M_\pi^2\right)^{1/2}$ and the factor $1/3$ appears because the three transverse directions are summed. Using the data from Table 1, $g_{\rho\pi\pi} = 6.08$ and $\Gamma_{\rho\pi\pi} = 0.151$ GeV are obtained, which is comparable to the Lattice results $g_{\rho\pi\pi} = 5.69(13)$ with $\Gamma_{\rho\pi\pi} = 0.155$ GeV [15] or the experimental data for $\rho^+ \to \pi^0\pi^+$ $\Gamma_{\rho\pi\pi} = 0.150 \pm 0.005$ GeV [16].

3 Electromagnetic decays of light and heavy pseudoscalar mesons

This section is devoted to the discussion of the electromagnetic decays and transition form factors for neutral pion and heavy η_c and η_b mesons.

The decay amplitude of the process $P \to \gamma\gamma$ is described by triangle Feynman diagram in Fig. 3 and reads as

$$T^{\mu\nu}(q_1, q_2) = N_c N_p \int \frac{dp}{(2\pi)^4} \varphi(p^2) \text{tr}\{i\gamma_5 S_i(p_2)\gamma_\mu S_i(p_3)\gamma_\nu S_i(p_1)\}. \tag{15}$$
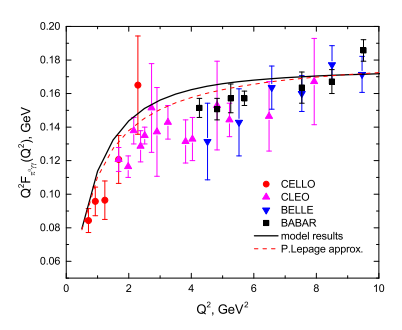
After applying the pion vertex function and taking the trace, the amplitude can be written as

$$\begin{aligned} T(q_1, q_2) &= i\epsilon_{\mu\nu\alpha\beta}\epsilon_1^\mu\epsilon_2^\nu q_1^\alpha q_2^\beta \left(N_c Q_q^2\right) \frac{mN_\pi}{4\pi^2} I(Q, q_1, q_2) = \\ &= i\epsilon_{\mu\nu\alpha\beta}\epsilon_1^\mu\epsilon_2^\nu q_1^\alpha q_2^\beta \left(N_c Q_q^2\right) G_{\pi\gamma\gamma}(Q, q_1, q_2), \end{aligned} \tag{16}$$

where q_1, q_2 are the photon momenta, Q_q is the quark charge, for the case with pion $Q_q^2 = (e_u^2 - e_d^2)$ and $e_u = 2/3e$, $e_d = -1/3e$.

The two - photon decay coupling constant in our model is obtained from Eq. (16) for two on-shell photons, when q_1^2 and q_2^2 are equal to zero.

$$g_{\pi\gamma\gamma} = G_{\pi\gamma\gamma}(M_\pi^2, 0, 0) \simeq \frac{mN_\pi}{4\pi^2\Lambda_\pi^2} I(M_\pi^2, 0, 0), \tag{17}$$
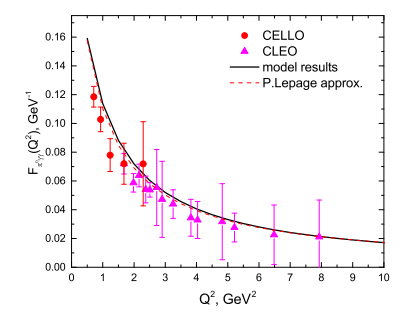
5

Figure 4: Transition form factor $F_{\pi\gamma}$ as a function of the space-like photon momentum Q^2. The experimental data are taken from [18–21].

then the decay width can be considered as

$$\Gamma(\pi^0 \to \gamma\gamma) = \frac{M_\pi^3}{64\pi}(4\pi\alpha)^2 g_{\pi\gamma\gamma}^2. \tag{18}$$

For the model parameters in Table. 1 the width $\Gamma_{\pi\gamma\gamma} = 7.76$ eV is obtained, and from the latest experiment it is known that $\Gamma_{\pi\gamma\gamma}^{\exp} = 7.82$ eV [17].

The transition form factor is calculated when one of the photons is supposed to be off-shell ($q_2^2 = -Q^2$), then it is defined as

$$F_{\pi\gamma}(Q^2) = e^2 G_{\pi\gamma\gamma}(M_\pi^2, Q^2, 0). \tag{19}$$

The pion electromagnetic decay has been widely studied experimentally and theoretically. The form factor $F_{\pi\gamma}(Q^2)$ was experimentally measured in e^+e colliders by the CELLO, CLEO, BaBar and Belle collaborations [18–21]. The latter two expanded the momentum transfer range from 4 to 40 GeV^2 and showed unexpected growth with increasing Q^2. The first theoretical estimation of the pion transition form factor as a function of the transferred momentum was made by S. Brodsky and P. Lepage within non-perturbative QCD [22]:
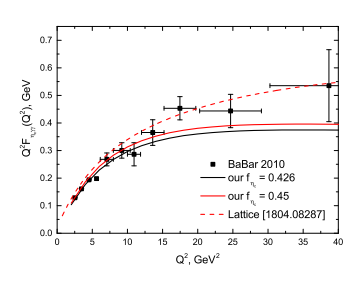
$$F_{\pi\gamma}(Q^2) = \frac{2f_\pi}{8\pi^2 f_\pi^2 + Q^2}, \tag{20}$$

which predicted the limit $Q^2 F_{\pi\gamma} = 2f_\pi$ at $Q^2 \to \infty$. The transition form factor $F_{\pi\gamma}(Q^2)$ as a function of Q^2 for our model is shown in Fig.4. The behaviour of the form factor demonstrates good agreement with the experimental data and the classical limit case in Eq.(20) (red dashed line).

To calculate the two-photon decay widths η_c and η_b, the quark masses $m_c = 1.6$ GeV and $m_b = 4.77$ GeV are fixed. The masses of the mesons, the scale parameters Λ_M, the decay constants and N_M are presented in Table 2. The decay widths $\Gamma_{\eta_{c(b)}\gamma\gamma}$ and the transition form factors are estimated using Eq. (18) and Eq.(19) with the replacement of the corresponding quark charge Q_q^2

6

	M_H, GeV	Λ_H, GeV	N_H	f_H (our)	f_H (refs)
η_c	2.985	2.775	3.546	0.426	0.42 [23]
η_b	9.39	2.81	8.568	0.715	0.705 [23]

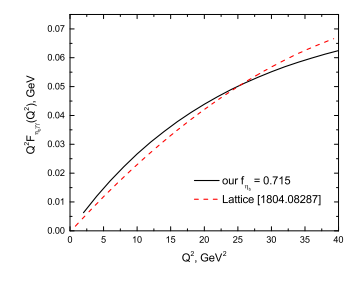Table 2: Model parameters and constants for heavy pseudoscalar mesons η_c and η_b.

Figure 5: Form factor $\eta_c\gamma\gamma$ and $\eta_b\gamma\gamma$ as function of the space-like photon momentum Q^2. The data are taken from [29] for η_c and from the light-front quark model for η_b [24].

as $4/9e^2$ and $1/9e^2$ respectively. For these parameters, the width of the decay $\eta_c \to \gamma\gamma$ is obtained as $\Gamma_{\eta_c\gamma\gamma} = 5.03$ keV. For comparison, the Lattice results range from 4.88 keV [24] to 6.788 keV [25] and PDG shows 5.1 ± 0.4 keV. For the η_b meson, the result $\Gamma_{\eta_b\gamma\gamma} = 0.18$ keV is obtained in the model. In other models, it varies from 0.17 keV in [26] to 0.659 ± 92 keV in [27] (see [28] for details).

The situation with the study of transition form factors and electromagnetic decays for η_c and η_b is worse both from the theoretical and experimental sides. For the charmonium case, the form factor $F_{\eta_c\gamma}(Q^2)$ was measured by the BaBar collaboration only in the space-like region up to 50 GeV^2 [29]. From the theoretical side, there exist descriptions of the η_c TFF in the space-like region in various theoretical approaches and phenomenological models such as pQCD [30], the light-front quark model [24], and the covariant approach based on Dyson-Schwinger and Bethe-Salpeter (BS) [31].

The left panel of Fig.5 illustrates the transition form factor $F_{\eta_c\gamma}$ for two values of the decay constant $f_{\eta_c} = 0.426$ and $f_{\eta_c} = 0.450$ and the experimental data are taken from [29]. Due to the absence of experimental data and poor theoretical investigations, in the right panel of Fig.5 the transition form factor $F_{\eta_b\gamma}$ is compared with the light-front quark model data taken from [24]. As can be seen, the best agreement between the experiment and the model appears at momenta $Q^2 < 15$ GeV^2.
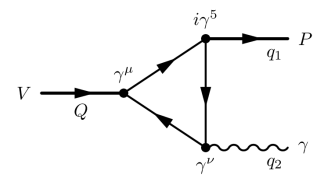
Figure 6: Feynman diagram of the $V \to P\gamma$ radiative decay.

4 Radiative decays of vector mesons

This section discusses the radiative decays of vector mesons into pseudoscalar mesons and photons. The decay $V \to P\gamma$ is defined by the Feynman diagram in Fig. 6 and the matrix element

$$T^{\mu\nu}(q_1, q_2) \quad = \quad N_c N_v N_p \int \frac{dp}{(2\pi)^4} \varphi(p^2) \text{tr}\{\gamma_\nu S_2(p_2) i\gamma_5 S_3(p_3)\gamma_\mu S_1(p_1)\}, \quad (21)$$

where $\varphi(p^2) = \varphi_v(p^2)\varphi_p(p^2)$. Then

$$T^{\mu\nu}(q_1, q_2) = i\epsilon_{\mu\nu\alpha\beta}\epsilon^\mu(Q)\epsilon_2^{*\nu}(q_2)Q^\alpha q_2^\beta \left(N_c Q_q e\right) \frac{m N_p N_v}{4\pi^2} I(Q, q_1, q_2). \quad (22)$$

The decay width is defined as

$$\Gamma_{VP\gamma} = \frac{1}{3}\alpha k^3 g_{VP\gamma}^2, \quad (23)$$

where $1/3$ appears due to vector polarizations, and the factor $k = (M_v^2 - M_p^2)/2M_v$.

Starting again from the light mesons and using the model data from Table 1 the radiative decay width for the light ρ meson is obtained as $\Gamma_{\rho\pi\gamma}$ =71.8 keV. This result is in agreement with the Lattice QCD result $\Gamma_{\rho\pi\gamma}$ =84.2(6.7)(4.3) keV [32] and the experimental data of 59.814 keV [16]. The calculation of the properties of heavy vector mesons is performed with the same quark masses as in the previous Section $m_c = 1.6$ GeV and $m_b = 4.77$ GeV. The masses of the mesons, parameters Λ_M, the decay constants and N_M are presented in Table 3.

	M_H, GeV	Λ_H, GeV	N_H	f_H (our)	f_H (refs)
J/ψ	3.075	2.03	3.238	0.435	0.399 [33]
Υ	9.405	4.22	3.489	0.705	

Table 3: Model parameters and constants for heavy quarkonia.

To evaluate the width of the decay processes $J/\psi \to \eta_c\gamma$, $\Upsilon \to \eta_b\gamma$, the appropriate vertices, masses, and quark charges should be used in Eq.(23). The process $\Upsilon \to \eta_b\gamma$ is studied in the framework of the light-front quark model [34],

where $\Gamma_{\Upsilon\eta_b\gamma} = 45$ eV and in the relativistic quark model [35], where $\Gamma_{\Upsilon\eta_b\gamma} = 5.8$ eV. The decay width $J/\psi \to \eta_c\gamma$ is obtained in Lattice QCD $\Gamma_{J/\psi\eta_s\gamma} = 2.219$ keV [25] and $\Gamma_{J/\psi\eta_s\gamma} = 2.49$ keV [36]. It was studied experimentally in the CLEO experiment ($\Gamma^{\text{exp}}_{J/\psi\eta_s\gamma} = 1.83$ keV) [37] and in the KEDR experiment ($\Gamma_{J/\psi\eta_s\gamma} = 2.17$ keV) [38]. The results obtained in our model are demonstrated in Table 4.

	our	refs.
$J/\psi \to \eta_c\gamma$	2.28 keV	1.83-2.49 keV (see text)
$\Upsilon \to \eta_b\gamma$	25.3 eV	5.8 [35], 45 eV [34]

Table 4: The radiative decay widths for heavy mesons.

5   Conclusions

In this work, an approach to describing properties of light and heavy mesons is developed in the framework of the effective quark model with nonlocal interaction. Models with nonlocal interaction are widely used to investigate the light- and heavy- flavoured mesons [7–10] at both zero and finite temperatures [11]. The nonlocality of quark-antiquark interaction is implemented in this model via the four-momentum Gaussian form factor in the meson vertex function. A set of model parameters, including the constituent quark masses and the meson size parameters Λ_H is obtained for light mesons and heavy mesons with hidden charm and bottom. The normalization constants N_H, which play the role of the meson-quark coupling, are obtained in explicit form. All the parameters are fixed via observables such as the meson mass and decay constants.

The model is applied to calculate the physical processes: decay of pseudoscalar mesons in two photons $\pi^0 \to \gamma\gamma$, $\eta_c \to \gamma\gamma$, $\eta_b \to \gamma\gamma$, the radiative decays of vector mesons $\rho \to \pi\gamma$, $J/\psi \to \eta_c\gamma$, $\Upsilon \to \eta_b\gamma$. All the results are consistent with the experimental data and the results of other models.

The advantage of this model is the simplicity of calculating one-loop integrals. The appendices provide further details needed for analytical analysis.

Appendix A: integration techniques

In order to demonstrate how the loop integrations in this work are carried out, let's start from the one-loop two-point integral:

$$I(P^2) = \int \frac{dp}{\pi^2} F(p^2) \frac{1}{[p_1^2 + m_1^2] [p_2^2 + m_2^2]}, \tag{24}$$

where $p_1 = p + q_1$ and $p_2 = p + q_2$ with $q_i = b_i P$ and $b_1 = -m_1/(m_1 + m_2)$, $b_2 = m_2/(m_1 + m_2)$, $b_2 - b_1 = 1$. The function $F(p^2)$ contains the vertex

functions $\varphi(-p^2/\Lambda_H^2)$. With the help of the Feynman parametrization we can write (**??**) as

$$I(P^2) = \int \frac{dp}{\pi^2} F(p^2) \int_0^1 d\alpha_1 \frac{1}{(\alpha_1(p_1^2 + m_1^2) + \alpha_2(p_2^2 + m_2^2))^2} \tag{25}$$

with $\alpha_2 = 1 - \alpha_1$.

The denominator in (25) is presented as

$$\alpha_1(p^2 + 2(pq_1) + q_1^2 + m_1^2) + \alpha_2(p^2 + 2(pq_2) + q_2^2 + m_2^2)$$
$$= (p + R)^2 + D \tag{26}$$

where $R = \sum_i \alpha_i q_i$ and $D = \sum_i \alpha_i(q_i^2 + m_i^2) - R^2$. It gives

$$I(P^2) = \int [d\alpha] \int \frac{dp}{\pi^2} F(p^2) \frac{1}{((p + R)^2 + D)^2} . \tag{27}$$

where $\int [d\alpha] = \int_0^1 d\alpha_1 \int_0^{1-\alpha_1} d\alpha_2 \delta(\alpha_1 + \alpha_1 - 1)$.

Using the integral representation in Euclidean space

$$\frac{1}{((p + R)^2 + D)^n} = \frac{1}{\Gamma(n)} \int t^{n-1} dt \, e^{-t((p+R)^2 + D)} . \tag{28}$$

and the Laplace transformation for the function $F(p^2)$:

$$\int s^n ds \tilde{F}(s) e^{-sz_0} = (-1)^n F^{(n)}(z_0) \tag{29}$$

the main integral Eq.(**??**) can be written as

$$I(P^2) = \int [d\alpha] ds \tilde{F}(s) t dt \int \frac{dp}{\pi^2} e^{-sp^2} e^{-t((p+R)^2 + D)} \tag{30}$$

Taking into account the relation

$$sp^2 + t((p + R)^2 + D) = (s + t)\left(p + \frac{t}{s+t} R\right)^2 + tD + \frac{st}{s+t} R^2 , \tag{31}$$

and changing the variables $t = st$ and using the inverse Laplace transformation:

$$\begin{aligned}
I(P^2) &= \int [d\alpha] \int ds \tilde{F}(s) \int t dt e^{-s(tD + \frac{t}{1+t} R^2)} \int \frac{dp}{\pi^2} e^{-s(1+t)p^2} \\
&= \int_0^1 d\alpha \int_0^\infty dt \frac{t}{(1+t)^2} [F(z_0)]
\end{aligned} \tag{32}$$

with

$$z_0 = tD + \frac{t}{1+t} R^2. \tag{33}$$

10

In general, after taking the traces during the Feynman diagram evaluation, not only scalar integrals appear. The most common expression for such integrals can be written as

$$\int \frac{dp}{\pi^2} F(p^2) \frac{\{p^\mu, p^\mu p^\nu, p^\mu p^\nu p^\rho, \ldots\}}{[p_1^2 + m_1^2][p_2^2 + m_2^2]}. \tag{34}$$

Calculation of vector and tensor integrals does not change the main idea in Eqs.(24-32)

$$\begin{aligned} I_\mu &= \int \frac{dp}{\pi^2} F(p^2) \frac{p^\mu}{[(p+q_1)^2 + m_1^2][(p+q_2)^2 + m_2^2]} = \\ &= -P^\mu \int_0^1 d\alpha(\alpha b_1 + (1-\alpha)b_2) \int_0^\infty dt \frac{t^2}{(1+t)^3}[F(z_0)]. \end{aligned} \tag{35}$$

The tensor integral

$$\begin{aligned} I_{\mu\nu} &= \int \frac{dp}{\pi^2} F(p^2) \frac{p^\mu p^\nu}{[(p+q_1)^2 + m_1^2][(p+q_2)^2 + m_2^2]}] \\ &= \frac{1}{2}\delta_{\mu\nu} \int_0^1 d\alpha \int_0^\infty dt \frac{t}{(1+t)^3} \int_0^\infty F(z_0 + u)du \\ &\quad + P^\mu P^\nu \int_0^1 d\alpha(\alpha b_1 + (1-\alpha)b_2)^2 \int_0^\infty dt \frac{t^3}{(1+t)^4}[-F'(z_0)]. \end{aligned} \tag{36}$$

The process of integration for integrals with a number of points more than two is carried out in the same way. And after applying the Feynman parametrization in Section 2 all results can be presented in terms of the integrals

$$I(a_0 \ldots a_n, m, n, F) = \int_0^1 \{d\alpha_i\} \prod_i \alpha_i^{a_i} \int_0^\infty dt \frac{t^m}{(1+t)^n}[F(z_0)]. \tag{37}$$

Appendix B: three point integrals

During the calculation of triangle diagrams set of integrals appears:

$$I(Q^2, q_1^2, q_2^2) = \int \frac{d^4 p}{\pi^2} F(p^2) \frac{\{1, p^\mu, p^{\mu\nu}, p^{\mu\nu\rho}\}}{(p_1^2 + m_1^2)(p_2^2 + m_2^2)(p_3^2 + m_3^2)}, \tag{38}$$

where $p_1 = p+q_1$ and $p_2 = p+q_2$, $p_3 = p+q_3$ with q_i defined from the kinematics of the process. The function $F(p^2)$ contains the sum of the vertex functions $\sum \varphi(-p^2/\Lambda_i^2)$. The procedure of integration is the same as in Appendix A and the results are presented below with notation $D_i = ((p+q_i)^2 + m_i^2)$:

$$\begin{aligned} I_3 &= \int \frac{dp}{\pi^2} F(p^2) \frac{1}{D_1 D_2 D_3} = \int_0^1 \{d\alpha_i\}\delta(1 - \sum \alpha_i) \int_0^\infty \frac{t^2}{(1+t)^2}[-F'[z_0]], \tag{39} \\ I_3^\mu &= \int \frac{dp}{\pi^2} F(p^2) \frac{p^\mu}{D_1 D_2 D_3} = \end{aligned}$$

11

$$= -\int_0^1 \{d\alpha_i\}\delta(1-\sum\alpha_i)R^\mu\int_0^\infty\frac{t^3}{(1+t)^3}[-F'[z_0]], \tag{40}$$

$$I_3^{\mu\nu} = \int\frac{dp}{\pi^2}F(p^2)\frac{p^\mu p^\nu}{D_1D_2D_3} =$$

$$= \frac{1}{2}\delta_{\mu\nu}\int_0^1\{d\alpha_i\}\delta(1-\sum\alpha_i)\int_0^\infty\frac{t^2}{(1+t)^3}F[z_0] +$$

$$+ \int_0^1\{d\alpha_i\}\delta(1-\sum\alpha_i)R^\mu R^\nu\int_0^\infty\frac{t^4}{(1+t)^4}[-F'[z_0]], \tag{41}$$

$$I_3^{\mu\nu\rho} = \int\frac{dp}{\pi^2}F(p^2)\frac{p^\mu p^\nu}{D_1D_2D_3} =$$

$$= -\frac{1}{2}\int_0^1\{d\alpha_i\}\delta(1-\sum\alpha_i)(R^\mu\delta^{\nu\rho}+R^\nu\delta^{\mu\rho}+R^\rho\delta^{\mu\nu})\int_0^\infty\frac{t^3}{(1+t)^4}F[z_0] -$$

$$- \int_0^1\{d\alpha_i\}\delta(1-\sum\alpha_i)R^\mu R^\nu R^\rho\int_0^\infty\frac{t^5}{(1+t)^5}[-F'[z_0]], \tag{42}$$

$$\tag{43}$$

where $R = \sum\alpha_i q_i$, $D = \sum\alpha_i(q_i^2 - m_i^2) - R^2$, z_0 is defined in Eq. (33), q_i depends on the kinematics of the process. For three-vertex diagram, up to three vertex functions $e^{-(p^2/\Lambda_i^2)}$ appear, and function

$$F(p^2) = exp\left(-p^2\sum_{n=1}^3\frac{1}{\Lambda_n^2}\right) = exp\left(-\frac{p^2}{\Lambda^2}\right) \tag{44}$$

with $\Lambda = \left(\sum_{n=1}^3\frac{1}{\Lambda_n^2}\right)^{-1/2}$.

References

[1] S. M. Schmidt, D. Blaschke and Y. L. Kalinovsky, Z. Phys. C **66** (1995) 485-490

[2] S. Leupold, Nucl. Phys. A **743** (2004) 283-302 [arXiv:hep-ph/0303020 [hep-ph]].

[3] U. Vogl, W. Weise, Prog. Part. Nucl. Phys. **27**, (1991) 195.

[4] K. Zalewski, Acta Phys. Polon. B **29** (1998) 2535-2538.

[5] Y. Burnier, O. Kaczmarek and A. Rothkopf, JHEP **12** (2015), 101 doi:10.1007/JHEP12(2015)101 [arXiv:1509.07366 [hep-ph]].

[6] G. T. Bodwin, E. Braaten and G. P. Lepage, Phys. Rev. D **51** (1995) 1125-1171 [erratum: Phys. Rev. D **55** (1997) 5853] [arXiv:hep-ph/9407339 [hep-ph]].

[7] T. Branz, A. Faessler, T. Gutsche, M. A. Ivanov, J. G. Korner and V. E. Lyubovitskij, Phys. Rev. D **81** (2010) 034010 [arXiv:0912.3710 [hep-ph]].

[8] C. T. Tran, M. A. Ivanov, P. Santorelli and H. C. Tran, Chin. Phys. C **49** (2025) 013111 [arXiv:2408.13776 [hep-ph]].

[9] S. Dubnička, A. Z. Dubničková, M. A. Ivanov, A. Liptaj, P. Santorelli and C. T. Tran, Phys. Rev. D **99** (2019) 014042 [arXiv:1808.06261 [hep-ph]].

[10] M. A. Ivanov, Y. L. Kalinovsky and C. D. Roberts, Phys. Rev. D **60** (1999), 034018 doi:10.1103/PhysRevD.60.034018 [arXiv:nucl-th/9812063 [nucl-th]].

[11] D. Blaschke, Y. L. Kalinovsky and P. C. Tandy, [arXiv:hep-ph/9811476 [hep-ph]].

[12] J. Gasser, H. Leutwyler, Physics Reports, Volume 87, Issue 3, 1982, Pages 77-169,

[13] P. Maris and P. C. Tandy, Phys. Rev. C, **60** (1999) 055214.

[14] B.K. Panda, S. Panda, S.N. Jena, A.K. Panda, Bulg. J. Phys. **50** (2023) 016-026. /

[15] C. Alexandrou, L. Leskovec, S. Meinel, J. Negele, S. Paul, M. Petschlies, A. Pochinsky, G. Rendon and S. Syritsyn, Phys. Rev. D **96** (2017) 034525 [arXiv:1704.05439 [hep-lat]].

[16] J. Huston, D. Berg, C. Chandlee, S. Cihangir, T. Ferbel, T, Jensen, C. Nelson Phys. Rev. D, **33**, (1986) 3199–3202.

[17] I. Larin *et al.* [PrimEx], Phys. Rev. Lett. **106** (2011) 162303 [arXiv:1009.1681 [nucl-ex]].

[18] B. Aubert *et al.* [BaBar Collaboration], Phys. Rev. D **80** (2009) 052002, [arXiv:0905.4778 [hep-ex]].

[19] S. Uehara *et al.* [Belle Collaboration], Phys. Rev. D **86** (2012) 092007, [arXiv:1205.3249 [hep-ex]].

[20] J. Gronberg *et al.* [CLEO], Phys. Rev. D **57** (1998) 33-54, [arXiv:hep-ex/9707031 [hep-ex]].

[21] Behrend, HJ., Criegee, L. et al [CELLO Collaboration], Z. Phys. C - Particles and Fields **49**, (1991) 401–409.

[22] S. Brodsky and P. G. Lepage, Phys. Rev. D **24**, (1981) 1808-1817.

[23] D. S. Hwang and G. H. Kim, Z. Phys. C **76** (1997) 107-110 [arXiv:hep-ph/9703364 [hep-ph]].

[24] H. Y. Ryu, H. M. Choi and C. R. Ji, Phys. Rev. D **98** (2018) 034018 [arXiv:1804.08287 [hep-ph]].

[25] B. Colquhoun *et al.* [Particle Data Group, HPQCD and (HPQCD Collaboration)‡], Phys. Rev. D **108** (2023) 014513 [arXiv:2305.06231 [hep-lat]].

[26] E. S. Ackleh, and T. Barnes, Phys. Rev. D, **45(1)** (1992) 232–240.

[27] A. A. Penin, A. Pineda, V. A. Smirnov and M. Steinhauser, Nucl. Phys. B **699** (2004) 183-206 [erratum: Nucl. Phys. B **829** (2010) 398-399] [arXiv:hep-ph/0406175 [hep-ph]].

[28] J. P. Lansberg and T. N. Pham, Phys. Rev. D **75** (2007) 017501 [arXiv:hep-ph/0609268 [hep-ph]].

[29] J. P. Lees *et al.* [BaBar], Phys. Rev. D **81** (2010) 052010 [arXiv:1002.3000 [hep-ex]].

[30] T. Feldmann and P. Kroll, Phys. Lett. B **413** (1997) 410-415 [arXiv:hep-ph/9709203 [hep-ph]].

[31] J. Chen, M. Ding, L. Chang and Y. x. Liu, Phys. Rev. D **95** (2017) 016010 [arXiv:1611.05960 [nucl-th]].

[32] L. Leskovec, C. Alexandrou, S. Meinel, J. W. Negele, S. Paul, M. Petschlies, A. Pochinsky, G. Rendon and S. Syritsyn, PoS **LATTICE2018** (2018) 065 [arXiv:1811.10034 [hep-lat]].

[33] J. J. Dudek, R. G. Edwards and D. G. Richards, Phys. Rev. D **73** (2006) 074507 [arXiv:hep-ph/0601137 [hep-ph]].

[34] H. M. Choi, J. Korean Phys. Soc. **53** (2008), 1205 [arXiv:0710.0714 [hep-ph]].

[35] D. Ebert, R. N. Faustov and V. O. Galkin, Phys. Rev. D **67** (2003) 014027 [arXiv:hep-ph/0210381 [hep-ph]].

[36] G. C. Donald, C. T. H. Davies, R. J. Dowdall, E. Follana, K. Hornbostel, J. Koponen, G. P. Lepage and C. McNeile, Phys. Rev. D **86** (2012) 094501 [arXiv:1208.2855 [hep-lat]].

[37] R. E. Mitchell *et al.* [CLEO], Phys. Rev. Lett. **102** (2009) 011801 [erratum: Phys. Rev. Lett. **106** (2011) 159903] [arXiv:0805.0252 [hep-ex]].

[38] V. V. Anashin, V. M. Aulchenko, E. M. Baldin, A. K. Barladyan, A. Y. Barnyakov, M. Y. Barnyakov, S. E. Baru, I. V. Bedny, O. L. Beloborodova and A. E. Blinov, *et al.* Chin. Phys. C **34** (2010), 831-835 [arXiv:1002.2071 [hep-ex]].